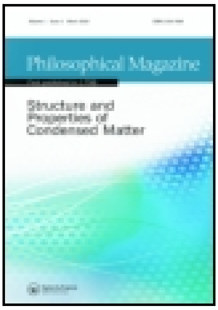

Philosophical Magazine
Publication details, including instructions for authors and subscription information:
http://www.tandfonline.com/loi/tphm20

Model of phase separation and of morphology evolution in two-phase alloy

V.V. Turlo [a] , A.M. Gusak [a] & K.N. Tu [b]

[a] Department of Physics, Cherkasy National University, Cherkasy, 18031, Ukraine

[b] Department of Materials Science and Engineering, University of California, Los Angeles, CA, USA

Version of record first published: 29 Nov 2012.

To cite this article: V.V. Turlo , A.M. Gusak & K.N. Tu (2012): Model of phase separation and of morphology evolution in two-phase alloy, Philosophical Magazine, DOI:10.1080/14786435.2012.747011

To link to this article: http://dx.doi.org/10.1080/14786435.2012.747011

Philosophical Magazine
2012, 1–13, iFirst Article

Model of phase separation and of morphology evolution in two-phase alloy

V.V. Turlo[a]*, A.M. Gusak[a] and K.N. Tu[b]

[a]*Department of Physics, Cherkasy National University, Cherkasy 18031, Ukraine;* [b]*Department of Materials Science and Engineering, University of California, Los Angeles, CA, USA*

(*Received 12 July 2012; final version received 31 October 2012*)

Elementary theory of mass-transfer in two-phase alloy under electromigration with account of two competing mechanisms of the fluxes equilibration is presented. These two competing mechanisms are Kirkendall effect and backstress. Various versions of Monte Carlo models for simultaneous simulation of structure evolution kinetics and of mass-transfer kinetics under high-density current are presented. Possibility of self-organization with minimization of Joule heating is demonstrated.

Keywords: electromigration; phase separation; backstress; Kirkendall effect; Monte Carlo simulation; entropy production; morphology

Introduction

Electromigration of ions in metals as a physical phenomenon was discovered at the end of 50s [1,2]. It became practically very important due to development of integrated circuits [3,4]. All integrated circuits include metallic interconnects (aluminium and copper) and solders (tin–lead or lead-free Sn–Bi, Sn–Ag–Cu and others). These metallic elements are, typically, less reliable than other elements – losing contact of metallic elements causes failures. To improve reliability of very large-scale integration devices, which means increase of mean time to failure, one must understand the main failure mechanisms. Most probable failure mechanisms are related to solder contacts. At that,

(1) solder is typically a two-phase alloy which can rather easily change its morphology and components spatial distribution under current;
(2) contacts of solders with other elements are the places of intermetallic phases formation (wavy or scallop-like layers of Cu_6Sn_5, Cu_3Sn_1 and Ni_3Sn_4). These intermetallic layers keep the contact. On the other hand, they are the most probable places of contact failures; and
(3) melting temperature is typically low (it is only 183 °C for classic eutectic tin–lead solder) – therefore there is a danger of local melting due to Joule heating.

---

*Corresponding author. Email: vladturlo@gmail.com

ISSN 1478-6435 print/ISSN 1478-6443 online

http://dx.doi.org/10.1080/14786435.2012.747011
http://www.tandfonline.com

Solder bumps providing solder contacts, say, in flip-chip technology, with size 50 microns, should be stable against passing current about 1 A, meaning current density $10^8 - 10^9\ \mathrm{A/m^2}$.

Often the failures are caused by electromigration in eutectic tin–lead. According to [5], after 100 h of current stressing with current density $8 \times 10^7\ \mathrm{A/m^2}$ at temperature 150 °C a pancake void at the cathode end was formed leading to failure. Moreover, as shown in [6–10], at temperatures higher than 100 °C the Pb atoms shift along electron motion direction (from cathode to anode) and Sn atoms shift in opposite direction. Hence, almost pure Pb segregated at the anode end, and almost pure Sn segregated at the cathode end. Thus, phase spatial separation in solder is driven by electric current.

Almost all solders are two-phase alloys. For example, eutectic tin–lead solder is a mixture of almost pure tin and weak solution of tin in lead with grain size about micron. Current stressing leads to:

- Joule heating;
- change of grain size (typically – coarsening, but recently possibility of grain refinement was discovered [11]);
- grain shape change (orientation along the current direction);
- component separation;
- accumulation and relaxation of stresses; and
- in many cases formation of sharp temperature gradients and, hence, thermomigration.

From fundamental point of view, very interesting (and still unsolved) is a problem of evolution path choice by the open system. Therefore, one of our aims is to find how the morphology evolution changes the entropy production or Joule heating.

Competition of backstress and Kirkendall effect in solder bumps

There are at least two major differences between electro- or thermomigration in aluminium thin films and in solder bumps:

1. Solders are typically two-phase binary or multicomponent structures and electro- or thermomigration causes redistribution of phase fractions and of components.
2. Electromigration induces stresses in aluminium films (backstress effect [3,12]), but not the Kirkendall effect (markers movement [13]). On the other hand, in solders we can see both effects – stress accumulation and marker movement.

In thin aluminium films, especially with bamboo structure, the lattice planes cannot move due to good adhesion with oxide layer and substrate, so Kirkendall effect is suppressed. Oxide layer covering the tin is not as rigid as aluminium oxide. Moreover, solder bumps are macroscopic, they contain many grains in the plane perpendicular to current. So, if even we imagine that the grains attached to oxide layer are immovable (like water in tube near the walls in hydrodynamic problem of liquid flow through cylindrical tube under fixed pressure difference), the more central grains can move as a whole, and it should be observed as marker movement.

This process of lattice movement should decrease the effect of stress accumulation. On the other hand, in the frame of non-equilibrium thermodynamics, lattice movement should be linearly linked to the driving force which is the stress gradient. Recently [14], we suggested the simplest form of such relation – velocity of lattice movement at time t in the place x is proportional to the local gradient of hydrostatic stress σ (one-third of the trace of the stress tensor):

$$U(t,x) = \eta\frac{\partial\sigma}{\partial x} = \kappa\frac{D_A^*}{kT}\,\Omega\,\frac{\partial\sigma}{\partial x}. \tag{1}$$

Here D_A^* is a tracer diffusivity, Ω is the atomic volume, $\eta/\Omega \equiv \kappa\frac{D_A^*}{kT}$ has a dimension of mobility and specially introduced unknown factor κ is non-dimensional, and it will be the main subject of our further considerations. Note that, though Equation (1) is formally similar to Nabarro-Herring creep [12], it is very different from it. NH-creep is caused by diffusion of individual vacancies or atoms, and velocity U in Equation (1) is a local velocity of lattice planes moving as a whole.

Let us make following assumptions:

1. Passing current is under threshold value – no whiskers, no hillocks, no voids so far.
2. Sinks and sources of vacancies are very effective so that local deviations of vacancy concentration from local equilibrium values are negligible. At the same time these equilibrium vacancy concentrations are non-uniformly distributed because of stress, which is not too high.
3. Vacancy volume is equal to atomic volume ($f=0$).
4. Geometry is planar, explicit influence of oxide film on closest regions is not taken into account.

Under these assumptions we can suggest one-dimensional 'Darken-like' description (since Darken never developed his famous phenomenological description [15] of interdiffusion for the case of two-phase alloys). This description, as well as original Darken's one, does not need explicit use of vacancies and takes into account the lattice drift without specification of its mechanism. Then equations for flux densities J_A, J_B of components can be written with simultaneous account of electron wind, backstress and Kirkendall flow:

$$\Omega J_A = \frac{C_A D_A^*}{kT}\,Z_A e\rho j_x + \frac{C_A D_A^*}{kT}\frac{\partial(\Omega\sigma)}{\partial x} + C_A U \tag{2a}$$

$$\Omega J_B = \frac{C_B D_B^*}{kT}\,Z_B e\rho j_x + \frac{C_B D_B^*}{kT}\frac{\partial(\Omega\sigma)}{\partial x} + C_B U \tag{2b}$$

(for the first two terms in both equations see, for example [10,16,17]) Here C_A, C_B are the atomic fractions of the components, $Z_A e, Z_B e$ are the effective charges of atoms under electromigration (with account of electron wind), kT is a Boltzmann constant times absolute temperature, j_x is a X-projection of electric current density and ρ is a mean specific resistance.

In Equation (1) for pure material, the tracer diffusivity is simply linked to vacancy diffusivity and vacancy concentration (fraction of empty sites): $D_A^* \approx C_V D_V$ (if one neglects correlation factor). In binary case this relation is generalized to the Frenkel equation: $C_V D_V \approx C_A D_A^* + C_B D_B^*$ (also neglecting correlation effect). Then, instead of Equation (1) in binary case, it seems natural to assume:

$$U = \kappa \frac{C_V D_V}{kT} \Omega \frac{\partial \sigma}{\partial x} = \kappa \frac{C_A D_A^* + C_B D_B^*}{kT} \Omega \frac{\partial \sigma}{\partial x} \tag{3}$$

Strictly speaking, so far the Equation (3) is no more than the definition of non-dimensional parameter κ. Yet, we will see below that the representation (3) of Kirkendall velocity is indeed convenient.

For undercritical regime, while voids and hillocks are not forming yet, in the laboratory reference frame, one has (completely similar to Darken in this respect)

$$J_A + J_B = 0 \tag{4}$$

Combining Equations (1)–(3), one gets:

$$\frac{C_V D_V}{kT} \frac{\partial(\Omega\sigma)}{\partial x} + \frac{C_A D_A^* Z_A + C_B D_B^* Z_B}{kT} e\rho j_x + U = 0 \tag{5}$$

$$\begin{aligned}(1+\kappa)\frac{C_V D_V}{kT} \frac{\partial(\Omega\sigma)}{\partial x} + \frac{C_A D_A^* Z_A + C_B D_B^* Z_B}{kT} e\rho j_x = 0 \Longrightarrow \frac{\partial(\Omega\sigma)}{\partial x} \\ = -\frac{1}{1+\kappa} \frac{C_A D_A^* Z_A + C_B D_B^* Z_B}{C_A D_A^* + C_B D_B^*} e\rho j_x \end{aligned} \tag{6}$$

It gives:

$$\Omega\, J_A = \frac{C_A C_B e\rho j_x}{kT(1+\kappa) C_V D_V} \left\{ \kappa C_V D_V (D_A^* Z_A - D_B^* Z_B) + (Z_A - Z_B) D_A^* D_B^* \right\} \tag{7}$$

$$J_B = -J_A$$

$$U = -\frac{\kappa}{1+\kappa} \frac{C_V D_V}{kT} \left(\frac{C_A D_A^* Z_A + C_B D_B^* Z_B}{C_V D_V} \right) e\rho j_x. \tag{8}$$

Case $\kappa \rightarrow 0$ means pure backstress. In this case

$$\Omega\, J_A = \frac{C_A C_B D_A^* D_B^*}{kT C_V D_V} (Z_A - Z_B)\, e\rho j_x \ = -\Omega\, J_B \quad U = 0 \tag{9}$$

Case $\kappa \rightarrow \infty$ means pure Kirkendall shift. In this case

$$\Omega\, J_A = \frac{C_A C_B}{kT}(D_A^* Z_A - D_B^* Z_B) e\rho j_x = -\Omega\, J_B\ ,\ U = -\left(\frac{C_A D_A^* Z_A + C_B D_B^* Z_B}{kT}\right) e\rho j_x. \quad (10)$$

Model

To simulate an electromigration, we constructed the Monte Carlo model based on exchange mechanism. In this model, atoms directly exchange places within the first coordination shell. Each exchange is realized or not realized according to common Metropolis algorithm. Of course, it is a distorted caricature of the real migration mechanisms in solders including vacancy jumps in the bulk and still discussed mechanisms of grain-boundary and inter-phase interface diffusion. Moreover, both components feel the electron wind force in the same direction. Nevertheless, external conditions of constant volume and shape (in undercritucal regime) provide compensating effects (backstress and Kirkendall effect) which equalize the fluxes of the components: namely, fluxes become opposite by direction and equal by magnitude [16].

For Monte Carlo simulation, the case of pure backstress at frozen Kirkendall effect is considered. According to Equation (9), in this case the effective diffusivity of both components is determined by Nernst–Planck diffusion coefficient $D = \frac{D_A^* D_B^*}{C_V D_V}$ and drift of both components (in opposite directions) is determined by the difference of effective charges $(Z_A - Z_B)$. For each possible elementary exchange, the change of energy ΔE is calculated. If $\Delta E<0$, then new configuration is accepted, else (if $\Delta E>0$), then a system obtains a chance of transition to new configuration: arbitrary value from the interval (0,1) is chosen randomly, if this value is less than $\mathrm{e}^{-\frac{\Delta E}{kT}}$, then new configuration is accepted, else a system stays in previous configuration.

So far, we simulated two-dimensional triangular lattice containing atoms *A* and *B* with average concentration 0.5. We introduced the pair interaction energies $\Phi_{AA}, \Phi_{AB}, \Phi_{BB}$ so that the decomposition criterion was fulfilled: $|\Phi_{AA}| + |\Phi_{BB}| > 2 \times |\Phi_{AB}|$.

Passing of electric current and corresponding electron wind on both components along with compensating backstress, described by Equation (9), necessitates the modification of energy change at elementary atomic exchange. Now it looks like: $\Delta E = \Delta E^{\phi} + \Delta E^{q}$, where ΔE^{ϕ} is an energy change related to pair interaction energies and ΔE^{q} is a change of energy related to the work of electric force and of backstress force during exchange. Naturally, only exchange of different species (*A* with *B*) is of interest for us:

$$\Delta E^q = \left(Z_A e\rho j_x + \Omega\,\frac{\partial\sigma}{\partial x}\right)\cdot\left(x_A^{\text{new}} - x_A^{\text{old}}\right) + \left(Z_B e\rho j_x + \Omega\,\frac{\partial\sigma}{\partial x}\right)\cdot\left(x_B^{\text{new}} - x_B^{\text{old}}\right). \quad (11)$$

Naturally,

$$\left(x_B^{\text{new}} - x_B^{\text{old}}\right) = -\left(x_A^{\text{new}} - x_A^{\text{old}}\right). \quad (12)$$

Then

$$\Delta E^q = (Z_A - Z_B)e\rho j_x \cdot (x_A^{\mathrm{new}} - x_A^{\mathrm{old}}) = \Delta Z \cdot e\rho j_x \cdot (x_A^{\mathrm{new}} - x_A^{\mathrm{old}}). \tag{13}$$

Here the resistivity is actually an average value: $\overline{\rho} = (\rho_A + \rho_B)/2$, where ρ_A and ρ_B are resistivities of pure A and B.

We started with a simple Model 1 in which the resistivity is taken as constant everywhere. Current density is taken unrealistically high (about $10^{12} - 10^{13}$ A/m^2); to obtain visible separation in reasonable computation time (Figure 1). Following parameters have been used:

$\Phi_{AA} = -4 \times 10^{-21}$ Joules, $\Phi_{AB} = -3 \times 10^{-21}$ Joules, $\Phi_{BB} = -5 \times 10^{-21}$ Joules, $\grave{O} = 300\widehat{E}$, $\overline{\rho} = 1 \times 10^{-6}\ \Omega$ m.

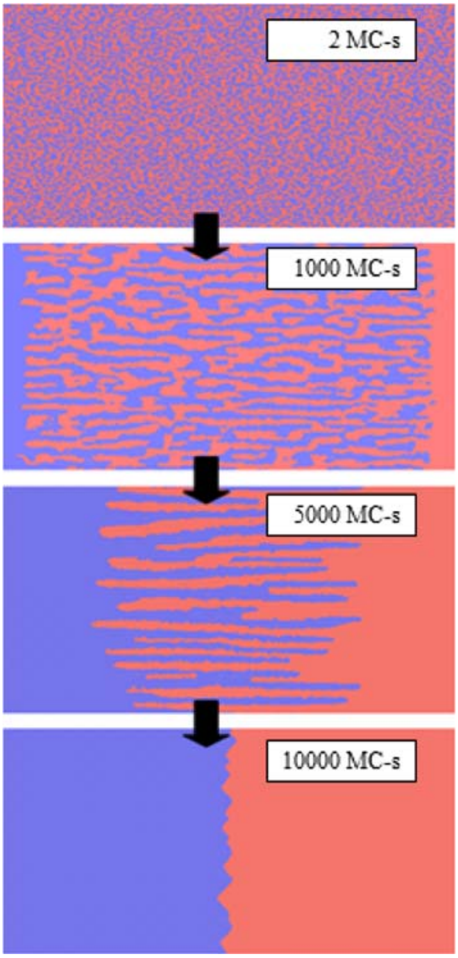

Figure 1. (colour online) Two-phase alloy morphology evolution at the uniform current distribution. The parameters of simulation are indicated in the text.

$$\Delta Z = 30 \times 10^{-19} C,\ j = 1 \times 10^{13}\ \mathrm{A/m^2}$$

Running of corresponding program demonstrated the elongation of A and B clusters along the current direction and also segregation of species at the boundaries. To compare our theoretical predictions with real experiment in Figure 2, we demonstrate experimental SEM views of morphology evolution [18].

We introduced a parameter of separation and found its dependence on the number of Monte Carlo steps (MCS) at various average current densities. Our choice of separation parameter was a difference between mass centres of A and B atoms: $\Delta x = \bar{x}_A - \bar{x}_B$, where

$$\bar{x}_A = \sum_{i=1}^{N_A} x_A[i]/N_A,\ \bar{x}_B = \sum_{i=1}^{N_B} x_B[i]/N_B. \tag{14}$$

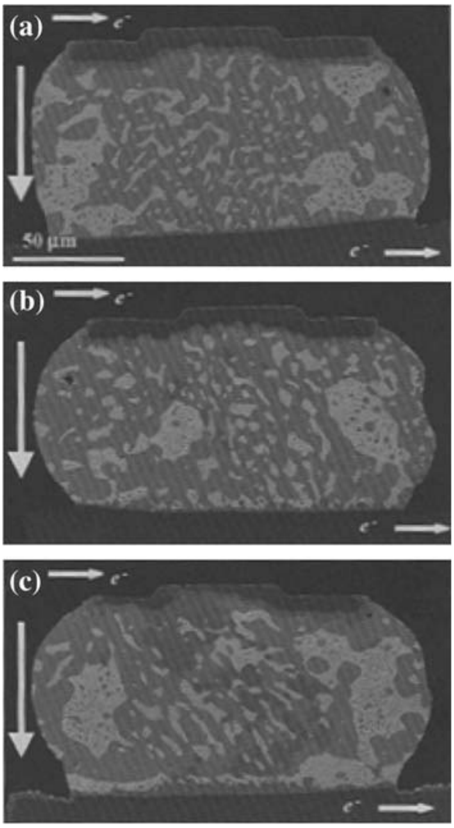

Figure 2. Eutectic tin–lead solder bump morphology evolution under average current density $3 \times 10^8\ \mathrm{A/m^2}$. SEM images taken after (a) 50 h, (b) 75 h and (c) 100 h of current stressing [18].

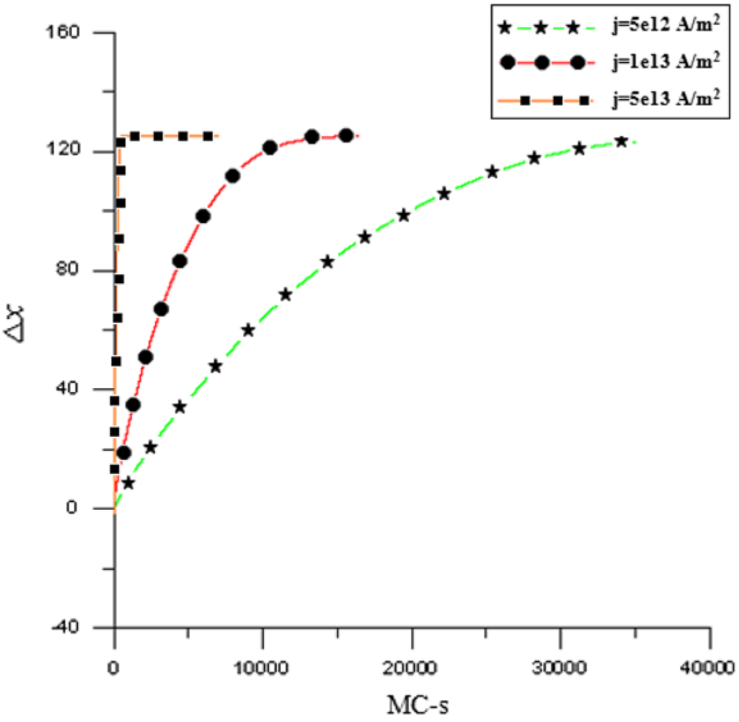

Figure 3. (colour online) Dependence of separation parameter on the MCS number at various average current densities.

MC time dependences of separation parameter are shown at Figure 3. All of them reach asymptotic value meaning full spatial phase separation.

The just described model is oversimplified since it neglects the local current density distribution and its feedback on the mass-transfer and structure evolution. So, our next step was to develop Model 2 taking into account the current distribution (see also [17]). The main idea is an application of first Kirchhoff's law (conservation of charge) and relation between electric field E and electric potential φ directly at the atomic scale

$$\mathrm{div}(\lambda E) = \mathrm{div}(\lambda \times \mathrm{grad}\varphi) = 0, \tag{15}$$

where divergence and gradient should be understood as the finite differences (λ is electric conductivity). Then for arbitrary ith site the following equation should hold:

$$\sum_{j=1}^{6} \lambda(i,j)(\varphi[j] - \varphi[i]) = 0, \tag{16}$$

where 6 is a number of neighbouring sites of each site in triangular lattice, j is an index of neighbouring site and $\lambda(i,j)$ is the electric conductivity between sites i and j, which is determined by the series connection formula for conductivities:

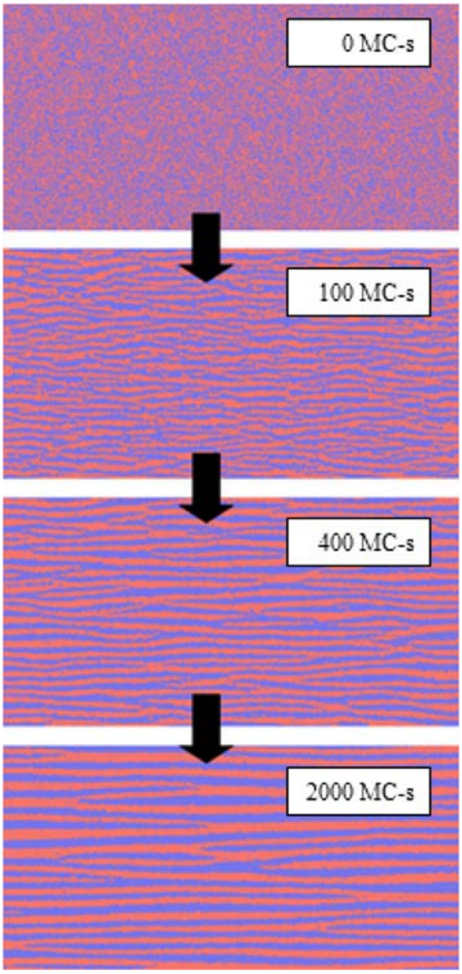

Figure 4. (colour online) Two-phase alloy morphology evolution at the non-uniform current distribution. The parameters of simulation are indicated in the text.

$$\lambda(i,j) = \frac{2 \times \lambda(i) \times \lambda(j)}{\lambda(i) + \lambda(j)}. \tag{17}$$

At that, if, say, site i is occupied by A atom and site j is occupied by B atom, then we take:

$$\lambda(i) = 1/\rho_{\mathrm{A}}, \lambda(j) = 1/\rho_{\mathrm{A}}.$$

Equation (16) can be solved by iteration procedure if we rewrite it in the following form:

$$\sum_{j=1}^{6} \lambda(i,j)(\phi^{(m)}[j] - \phi^{(m+1)}[i]) = 0, \tag{18}$$

where m is a previous iteration and $m+1$ is a next iteration step. Then,

$$\varphi^{(m+1)}[i] = \frac{\sum_{j=1}^{6} \lambda(i,j) \times \varphi^{(m)}[j]}{\sum_{j=1}^{6} \lambda(i,j)}. \tag{19}$$

After finding potential in each site, we renormalize it so that average current density (or total current) remains fixed. To do this, we take the two marginal atomic planes perpendicular to total current flow and find that:

$$j^{\mathrm{real}} = \Big(\sum_{j:=0}^{ny} \lambda_j(n,n-1) \times (\varphi_j[n] - \varphi_j[n-1])\Big)/(dx \times ny), \tag{20}$$

where j is a number of 'plane' (actually, row) parallel to total current flow. Then, we renormalize the potentials in the following way:

$$\varphi^{\mathrm{renorm}}[i] = \varphi[i] \times \frac{j}{j^{\mathrm{real}}}. \tag{21}$$

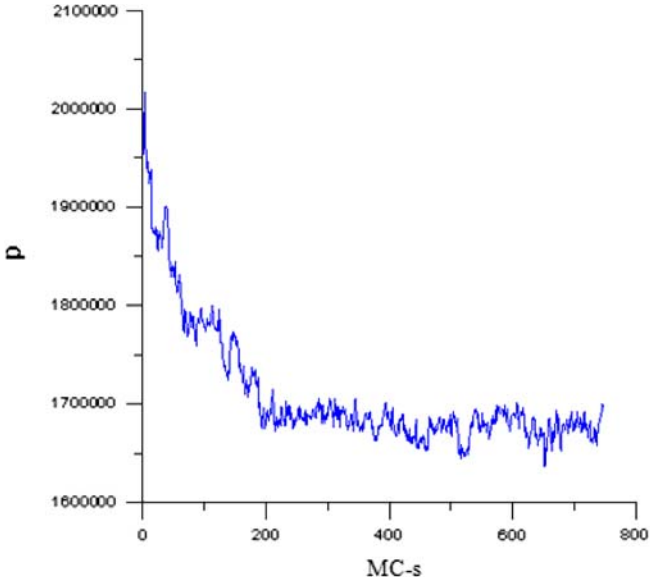

Figure 5. (colour online) Dependence of p-parameter (actually, of Joule heating and of entropy production) on Monte Carlo time at $j = 1 \times 10^{13}$ A/m^2.

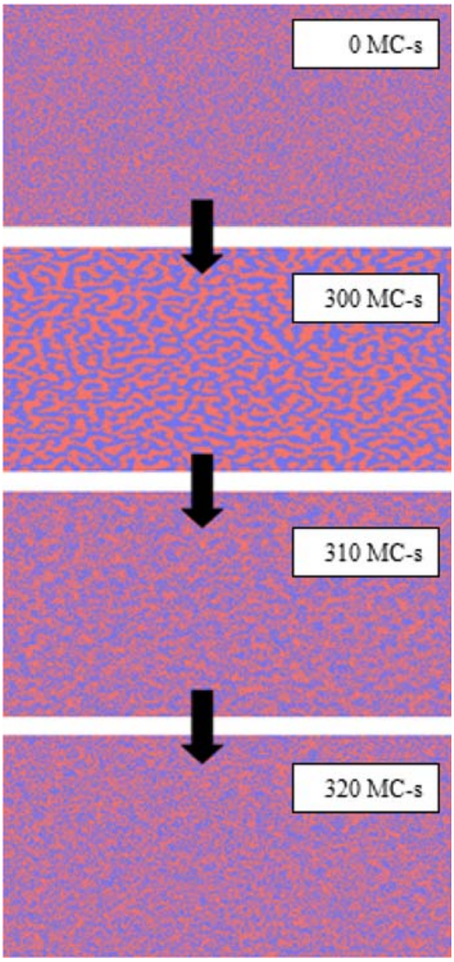

Figure 6. (colour online) Refinement of grains (clusters) under high current density – results of Monte Carlo simulation, parameters are indicated in the text.

Simulation demonstrates (Figure 4) enlargement and elongation of *A* and *B* clusters which lets system to reduce the total resistance (actually, it is a transfer to parallel connection).

To quantify this process, we introduced the parameter $p = \sum_{i=1}^{n} \sum_{j=1}^{6} \lambda(i,j)(\phi[i] - \phi[j])^2$. This parameter is proportional to the Joule heating intensity.

Dependence of p-parameter on Monte Carlo time at average current density $j = 1 \times 10^{13}\ \mathrm{A/m^2}$ is shown at Figure 5.

This result seems important from the fundamental point of view. It means that the open system under current is self-organizing in such a way, that the energy dissipation tends to minimum. This result correlates with well-known principles of non-equilibrium thermodynamics of the open systems [19].

We also studied the possibility of grains refinement under current stressing. For this, we started MC simulations at first without current and obtained usual decomposition picture with some average grain size. After that we switched on a current $10^{14}\ \mathrm{A/m^2}$). We observed refinement and elongation of grains instead of their growth (Figure 6).

Summary

1. Equalizing of fluxes under electric current through two-phase solder in undercritical regime (without formation of voids and hillocks) can be provided by backstress, by Kirkendall flow or by their combination.
2. Separation rate can be presented as a superposition of backstress-driven rate and Kirkendall-driven rate. First one is proportional to the difference of effective charges and to Nernst–Planck diffusivity and second one is proportional to the difference of products of effective charges and tracer diffusivities.
3. If simulation of mass-transfer in solder under current neglects the redistribution of current, then one obtains vivid phase separation and structure coarsening without vivid texture.
4. If simulation of mass-transfer in solder under current takes the redistribution of current and electric potential into account (self-consistent problem), then one two-phase alloy forms the elongated grains demonstrating transition to parallel connection of phases.
5. At that the Joule heating and entropy production tend to minimum.
6. If after grains coarsening without current, one switches on high current density, a grain refinement is observed. To the best of our knowledge, it is a first computer simulation of the effect which had been recently discovered experimentally [11,16].

Acknowledgements

The work is supported by The State Fund for Fundamental Researches of Ukraine (Project F40.7/040) and by Ministry of Education and Science of Ukraine.

References

[1] V.B. Fix, *Ionic Conduction in Metals and Semiconductors*, Nauka, Moscow, 1969.
[2] H.B. Huntington and A.R. Grone, J. Phys. Chem. Solids. 20 (1961) p.76.
[3] I.A. Blech, J. Appl. Phys. 47 (1976) p.1203.
[4] J.R. Black, Proc. IEEE. 57 (1969) p.1587.
[5] S. Brandenburg and S. Yeh, *SMI98*, CA, San Jose, CA. 337, 1998.
[6] C.Y. Liu, C. Chen, C.N. Liao and K.N. Tu, Appl. Phys. Lett. 75 (1999) p.58.
[7] C.Y. Liu, C. Chen and K.N. Tu, J. Appl. Phys. 88 (2000) p.5703.
[8] T.Y. Lee, K.N. Tu, S.M. Kuo and D.R. Frear, J. Appl. Phys. 89 (2001) p.3189.
[9] T.Y. Lee, K.N. Tu and D.R. Frear, J. Appl. Phys. 90 (2001) p.4502.
[10] K.N. Tu, J. Appl. Phys. 94 (2003) p.5451.
[11] F.Y. Ouyang, K.N. Tu, Y.S. Lai and A.M. Gusak, Appl. Phys. Lett. 89 (2006) p.221906.

[12] K.N. Tu, J.W. Mayer, L.C. Feldman, *Electronic Thin Film Science: For Electrical Engineers and Materials Scientists*, New York, NY, Macmillan, 1992.

[13] A.D. Smigelskas and E.O. Kirkendall, Trans. AIME. 171 (1947) p.130.

[14] A.M. Gusak, N.V. Tyutyunnyk and K.N. Tu, Defect Diffus. Forum. (2011) p.309.

[15] L.S. Darken, Trans. Met. Soc. AIME. 175 (1948) p.184.

[16] K.N. Tu, *Electronic Thin-Film Reliability*, Cambridge University Press, New York, NY, 2011.

[17] T.V. Zaporozhets, A.M. Gusak, K.N. Tu and S.G. Mhaisalkar, J. Appl. Phys. 98 (2005) p.103508.

[18] K.N. Tu, *Solder Joint Technology: Materials, Properties, and Reliability*, New York, NY, Springer, 2007.

[19] A.M. Gusak, T.V. Zaporozhets, Yu.O. Lyashenko, S.V. Kornienko, M.O. Pasichnyy and A.S. Shirinyan, *Diffusion-controlled Solid State Reactions in Alloys, Thin-Films, and Nanosystems*, Wiley-VCH, Berlin, Ch. 11, 2010.